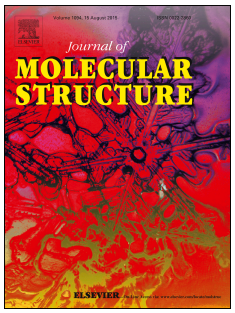

Benzenesulfonohydrazides inhibiting urease: Design, synthesis, their in vitro and *in silico* studies

Mahmood Ahmed, Muhammad Imran, Muhammad Muddassar, Riaz Hussain, Muhammad Usman Khan, Saghir Ahmad, Muhammad Yasir Mehboob, Saira Ashfaq

PII: S0022-2860(20)31065-6

DOI: https://doi.org/10.1016/j.molstruc.2020.128740

Reference: MOLSTR 128740

To appear in: *Journal of Molecular Structure*

Received Date: 25 February 2020

Revised Date: 9 June 2020

Accepted Date: 21 June 2020

Please cite this article as: M. Ahmed, M. Imran, M. Muddassar, R. Hussain, M.U. Khan, S. Ahmad, M.Y. Mehboob, S. Ashfaq, Benzenesulfonohydrazides inhibiting urease: Design, synthesis, their in vitro and *in silico* studies, *Journal of Molecular Structure* (2020), doi: https://doi.org/10.1016/j.molstruc.2020.128740.

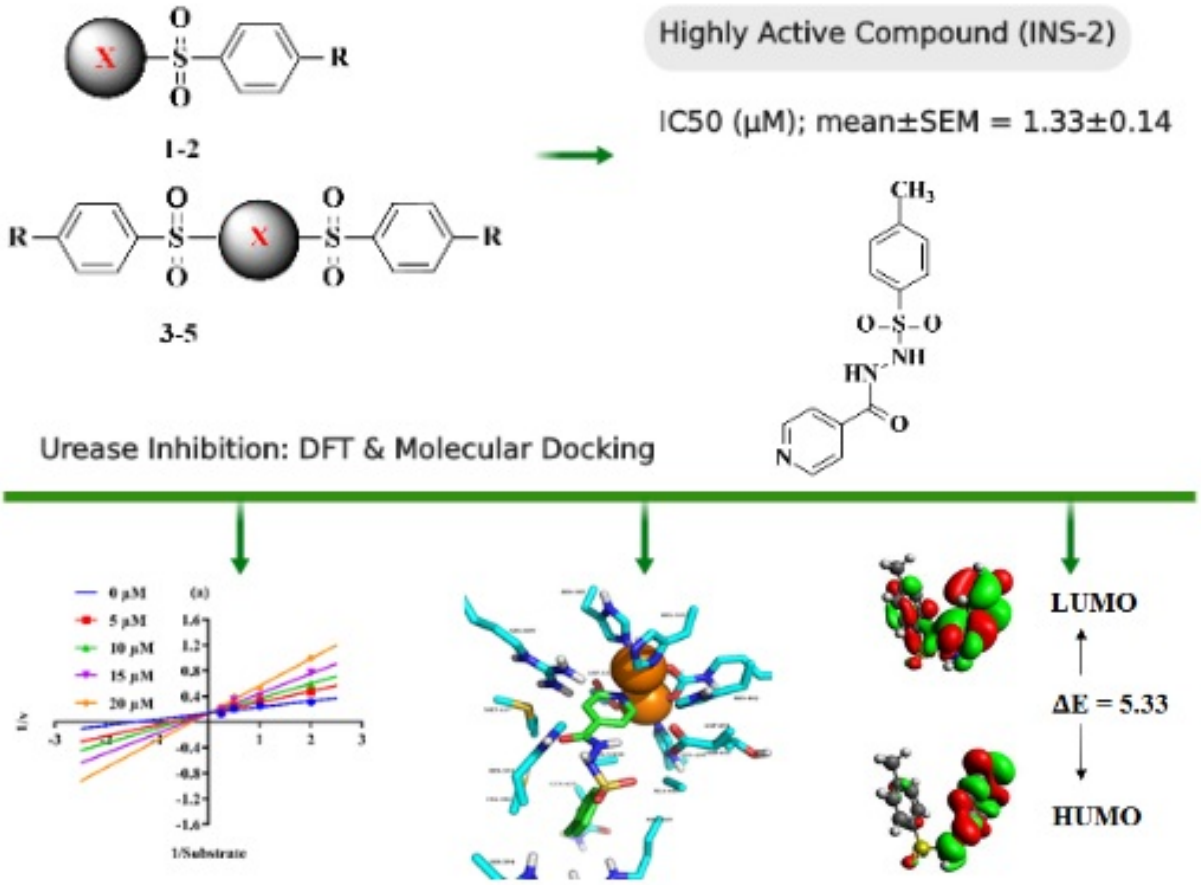
1-2
3-5
Highly Active Compound (INS-2)
IC50 (μM); mean±SEM = 1.33±0.14
Urease Inhibition: DFT & Molecular Docking
0 μM
5 μM
10 μM
15 μM
20 μM
1/Substrate
LUMO
ΔE = 5.33
HUMO

Benzenesulfonohydrazides inhibiting urease: Design, synthesis, their *in vitro* and *in silico* studies

Mahmood Ahmed [1*], Muhammad Imran [2], Muhammad Muddassar [3], Riaz Hussain [4], Muhammad Usman Khan [4,5], Saghir Ahmad [6], Muhammad Yasir Mehboob [4], Saira Ashfaq[2]

[1] Renacon Pharma Limited, Lahore 54600, Pakistan

[2] School of Life Sciences, FC College (A Chartered University) Lahore- Pakistan

[3] Department of Biosciences, COMSATS University, Park Road, Islamabad- Pakistan

[4] Department of Chemistry, University of Okara, Okara-56300, Pakistan

[5] Department of Applied Chemistry, Government College University, Faisalabad-38000, Pakistan

[6] Institute of Chemistry, University of the Punjab. Lahore 54590, Pakistan

Running title: Benzenesulfonohydrazide as urease inhibitors

To whom correspondence should be addressed

Dr. Mahmood Ahmed

mahmoodresearchscholar@gmail.com

Abstract

Keeping in view the therapeutic importance of ureases due to its involvement in different pathological conditions, its inhibition was investigated by newly synthesized benzenesulfonohydrazides. Elemental analysis, IR, ^{1}H NMR and ^{13}C NMR spectral studies were performed to elucidate the structure of benzenesulfonohydrazides. In vitro urease enzyme inhibition assay revealed the compound INS-5 was found to be the most potent (IC_{50} = 1.11±0.29µM) among the tested compounds. The compound INS-2 was competitive inhibitor with Ki value 5.60 µM while the compounds INS-1 and INS-5 were mixed type of inhibitors with Ki values 4.32 and 2.76 µM respectively. Ancillary to synthetic studies, DFT and TDDFT calculations at B3LYP/6-311G(d,p) level of theory were performed for comparative analysis of spectroscopic data, frontier molecular orbitals (FMOs), natural bond orbital (NBO) analysis and molecule electrostatic potential (MEP) surface. Overall, experimental findings were supported nicely by corresponding DFT computed results. The NBO analysis confirmed that the presence of hyperconjugative interactions are pivotal cause for stability of investigated compounds. Global reactivity descriptors were also calculated using the energies of FMOs energies. Molecular docking studies were performed to identify the plausible binding mode of the competitive inhibitor.

Keywords: Hydrazide; Isonicotinoyl; Urease; DFT; Docking studies

1. Introduction

Urease is a metalloenzyme (nickel based, urea amidohydrolase, EC 3.5.1.5) which belongs to super family of aminohydrolase and phosphotriesterase that accelerate the transformation of urea into carbon dioxide and ammonia. Canavaliaensiformis (jack bean) was first well characterized and crystalize among the numerous ureases that is utilized in enzyme inhibition studies. Continuous formation of ammonia enhances the gastric mucosa permeability that results in inflammation, ulcer, adenocarcinoma and lymphoma [1-5]. *Helicobacter pylori*(*H. pylori*) relies on urease activity for bacterial survival in low pH environment of the stomach, therefore targeting urease activity can eradicate the bacterium in early stages of the infection[6, 7]. Since the structure, molecular weight, amino acid sequence of urease greatly depends upon its origin. The bacterial ureases are heteropolymeric molecules having three subunits, α, β and γ whereas the urease from jack beans are homohexameric molecules having six α subunits. Despite the difference in the structure, the active site of the enzyme, largely remains conserved. The active site is always located in α subunits having binuclear nickel center[8, 9]. Due to involvement of urease in bacterial infections, designing of novel urease inhibitors are of great research interest. The current eminence of urease inhibitors is quite restricted. However mostly five different classes of inhibitors including barbituric acid analogues [10], thiourea derivatives [11], five and six-membered heterocyclics, natural products and metal complexes are available in literature [12] but these are not efficient with regard their drug like properties and the full potential of urease inhibition is yet to be discovered. Hydrazide moiety along

with heterocyclics and sulfoxide exhibits a wide range of biological activities including antibacterial, antifungal, antinociceptive, anticonvulsant, enzyme inhibition and anticancer [10, 13-15]. In literature, hydrazides as sulfonohydrazides [16], hydrazide-carbazoles [17] and hydrazide-hydrazones [18] are reported for their cytotoxic activities. Sulfonohydrazides had shown the cytotoxic effect against brain and ovarian tumor cells and inhibited the cell proliferation at < 10 µM concentration. Hydrazides integrated carbazoles revealed a significant cytotoxic effect against the pancreatic cell lines(AsPC1 and SW1990) with IC_{50} values ranged between 3.42-22.42 µM whereas hydrazide-hydrazone derivatives showed the cytotoxic effect against colon, gastric and hepatoma carcinoma cells and displayed higher cytotoxic activity than 5-fluorouracil. So in struggle to identify lead molecules for enzyme inhibition by our research group, we are reporting synthesis and urease inhibitory activities of new hydrazides (Fig. 1) on the basis of their wide range biological activities. Due to the involvement of ureases in different pathological conditions, the discovery of safe and potent urease inhibitors has been an area of challenge in pharmaceutical research. Additionally density functional theory (DFT) calculations have been performed to evaluate spectroscopic (FT-IR and UV-Visible) studies, frontier molecular orbital (FMO) analysis, natural bond orbital (NBO) analysis, global reactivity parameters and molecular electrostatic potential (MEP) surfaces properties of investigated compounds. Enzyme kinetics and molecular modeling studies were also carried out to get insight into inhibition mechanism and binding conformation of competitive inhibitor in urease enzyme.

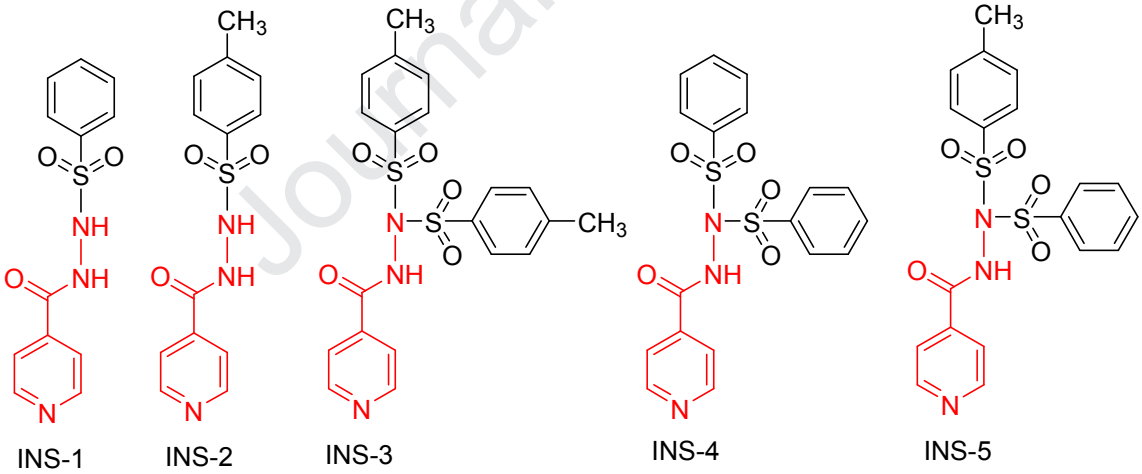

Fig. 1 Benzenesulfonohydrazide under investigation

2. Experimental

In this research high purity chemicals were used and these were acquired from Falcon Scientific, Lahore-Pakistan originate to Merck (Germany) whereas high purity water was produced in our own lab using Milli-Q® water system (UK). Spectral studies including IR (FTIR spectrophotometer, Agilent Technologies, Carry 630), ^{1}HNMR-500 MHz, ^{13}CNMR-125 MHz (NMR spectrometer, Bruker, USA) and elemental analysis (C, H, N and S by Flash elemental analyzer, HT+ Thermo

Scientific, UK) were performed to elucidate the structure of newly synthesized compounds. Melting point was determined by Gallenkamp apparatus and PG-T80UV-Vis spectrophotometer (PG, Instruments-UK) was used to calculate λ_{max}. Pre-coated silica plates (Merck, Germany) were spotted for TLC analysis and spots were detected in UV light to confirm the purity of the synthesized compounds.

2.1. Protocol for benzenesulfonohydrazide synthesis

A most convenient route under dynamic pH control in an aqueous medium was used for the synthesis of sulfonamides already described in our earlier work [19-21] and details are explained in supplementary data. Details chemistry for synthesis of compounds 1-5 with physiochemical and spectral data explained below.

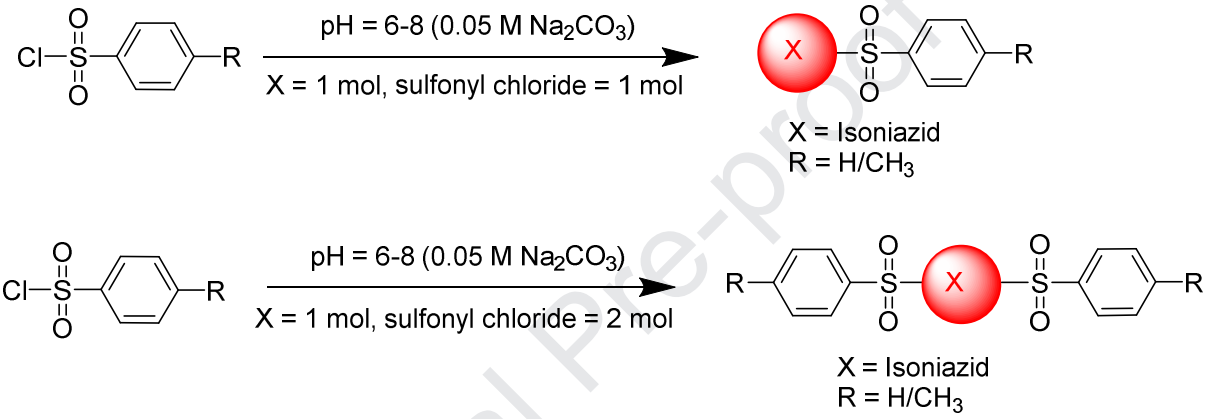

Scheme 1. Synthesis of Benzenesulfonohydrazide

2.1.1. *N'*-isonicotinoylbenzenesulfonohydrazide (INS-1)

White solid; Yield, 79.4 %; M. P., 112-114°C; R_f, 0.76. UV λ_{max} (nm): 242.IR (ATR, υ cm^{-1}): 3567, 3247 (N-H), 3057 (CH-aromatic), 1681 (C=O), 1307 (-SO_2-$NH_{2\text{-asym}}$), 1154 (-SO_2-$NH_{2\text{-sym}}$), 1091 (-S=O). ^{1}H NMR (500 MHz, DMSO-d_6): δ_H 8.89 (2H, d, J = 7.6 Hz, CH-pyridyl), 8.08 (1H, s, -NH-CO), 7.56-7.84, (7H, m, ArH), 2.32 (1H, s, -NH). ^{13}C NMR (125 MHz, DMSO-d_6): 165.8, 149.0, 141.9, 140.3, 136.6, 131.0, 129.7, 127.7.Anal. Calc. for $C_{12}H_{11}N_3O_3S$ (FW=277.3 g/mol): C, 51.98; H, 4.0; N, 15.15; S, 11.56 %. Found: C, 51.81; H, 3.89; N, 15.37; S, 11.45%.

2.1.2. *N'*-isonicotinoyl-4-methylbenzenesulfonohydrazide (INS-2)

White solid; Yield, 94.2 %; M. P., 180-182°C; R_f, 0.79. UV λ_{max} (nm): 242.IR (ATR, υ cm^{-1}): 3572, 3244 (N-H), 3057 (CH-aromatic), 1676 (C=O), 1337 (-SO_2-$NH_{2\text{-asym}}$), 1157 (-SO_2-$NH_{2\text{-sym}}$), 1090 (-S=O). ^{1}H NMR (500 MHz, DMSO-d_6): δ_H 8.89 (2H, d,J = 7.6 Hz, CH-pyridyl), 8.02 (1H, s, -NH-CO), 7.74-7.84, (4H, m, ArH), 7.40 (2H, d, J = 7.5Hz,ArH), 2.32 (3H, s, CH_3), 2.12 (1H, s, -NH). ^{13}C NMR (125 MHz, DMSO-d_6): 165.8, 149.0, 141.9, 140.3, 136.6, 131.0, 129.7, 127.7, 21.3 (-CH_3). Anal. Calc. for $C_{13}H_{13}N_3O_3S$ (FW=291.3 g/mol): C, 53.60; H, 4.50; N, 14.42; S, 11.01 %. Found: C, 53.86; H, 4.69; N, 14.57; S, 11.15 %.

2.1.3. *N′*-isonicotinoyl-4-methyl-N-tosylbenzenesulfonohydrazide (INS-3)

Yellowish white solid; Yield, 82.2 %; M. P., 174-176°C; R_f, 0.81. UV λ_{max} (nm): 235.IR (ATR, υ cm^{-1}): 3565, 3242 (N-H), 3054 (CH-aromatic), 1676 (C=O), 1336 ($-SO_2-NH_{2-asym}$), 1158 ($-SO_2-NH_{2-sym}$), 1089 (-S=O). ^{1}H NMR (500 MHz, DMSO-d_6): δ_H 8.89 (2H, d,*J* = 7.6 Hz, CH-pyridyl), 8.02 (1H, s, -NH-CO), 7.74-7.81, (6H, m, ArH), 7.40 (4H, d, *J* = 7.5Hz,ArH), 2.32 (6H, s, 2 x CH_3). ^{13}C NMR (125 MHz, DMSO-d_6): 164.8, 149.0, 141.9, 140.3, 136.6, 131.0, 129.7, 127.7, 21.3 (2 x CH_3). Anal. Calc. for $C_{20}H_{19}N_3O_5S_2$ (FW=445.5 g/mol): C, 53.92; H, 4.30; N, 9.43; S, 14.39 %. Found: C, 53.86; H, 4.61; N, 9.54; S, 13.45 %.

2.1.4. *N′*-isonicotinoyl-N-(phenylsulfonyl)benzenesulfonohydrazide (INS-4)

Yellowish white solid; Yield, 75.5 %; M. P., 120-122°C; R_f, 0.67. UV λ_{max} (nm): 235.IR (ATR, υ cm^{-1}): 3572, 3244 (N-H), 3056 (CH-aromatic), 1676 (C=O), 1337 ($-SO_2-NH_{2-asym}$), 1157 ($-SO_2-NH_{2-sym}$), 1090 (-S=O). ^{1}H NMR (500 MHz, DMSO-d_6): δ_H 8.87 (2H, d, *J* = 7.6 Hz, CH-pyridyl), 8.02 (1H, s, -NH-CO), 7.81-7.86, (6H, m, ArH), 7.71 (2H, d, *J* = 7.4Hz,ArH), 7.62 (2H, d, *J* = 7.5Hz,ArH). ^{13}C NMR (125 MHz, DMSO-d_6): 164.0, 149.0, 141.0, 140.0, 139.6, 131.0, 129.7, 127.0. Anal. Calc. for $C_{18}H_{15}N_3O_5S_2$ (FW=417.5 g/mol): C, 51.79; H, 3.62; N, 10.07; S, 15.36 %. Found: C, 51.90; H, 3.51; N, 10.14; S, 15.48%.

2.1.5. *N′*-isonicotinoyl-4-methyl-N-(phenylsulfonyl)benzenesulfonohydrazide (INS-5)

Yellowish white solid; Yield, 93.8 %; M. P., 162-164°C; R_f, 0.86. UV λ_{max} (nm): 242.IR (ATR, υ cm^{-1}): 3565, 3248 (N-H), 3055 (CH-aromatic), 1676 (C=O), 1336 ($-SO_2-NH_{2-asym}$), 1156 ($-SO_2-NH_{2-sym}$), 1090 (-S=O). ^{1}H NMR (500 MHz, DMSO-d_6): δ_H 8.88 (2H, d,*J* = 7.6 Hz, CH-pyridyl), 8.04 (1H, s, -NH-CO), 7.74-7.81, (9H, m, ArH), 7.40 (2H, d, *J* = 7.5Hz,ArH), 2.32 (3H, s, CH_3). ^{13}C NMR (125 MHz, DMSO-d_6): 164.2, 149.0, 141.0, 140.3, 136.2, 131.0, 129.6, 127.7, 21.3 (CH_3). Anal. Calc. for $C_{19}H_{17}N_3O_5S_2$ (FW=431.5 g/mol): C, 52.89; H, 3.97; N, 9.74; S, 14.86 %. Found: C, 52.86; H, 3.71; N, 7.58; S, 14.65 %.

2.2. % Urease inhibition assay, IC_{50} and kinetics study protocol

Urease inhibition assay was performed as reported in our earlier studies [22] and details are provided in supplementary data.

2.3. Computational studies

The overall quantum chemical calculations are performed with the help of DFT employing Gaussian 09 program package[23]. Geometrical optimization was done without symmetry restrictions by applying B3LYP level of DFT and 6-311G (d,p) basis set combination. The frequency analysis based on DFT/B3LYP/6-311G (d,p) level of theory was used for confirmation of stability associated with the optimized geometries. The absence of negative eigen values among all calculated frequencies reflected that optimized geometries of INS-1-INS-5 correspond to true minimum at potential energy surfaces. The frontier molecular orbital and molecule electrostatic potential analysis was conducted at

B3LYP level of DFT and 6-311G (d,p) basis set conjunction. The NBO analysis was carried out at B3LYP/6-311G (d,p) level of theory using NBO 3.1 program package. The UV-Vis analysis was performed employing time dependent density functional theory (TDDFT) calculations at B3LYP/6-311+G (d,p) level of theory for estimation of photophysical characteristics of INS-1-INS-5. Furthermore, the frequency analysis based on DFT/B3LYP/6-311G(d,p) level of theory was used for confirmation of stability associated with the optimized geometries. The absence of negative eigen values among all calculated frequencies reflected that optimized geometries of INS-1-INS-5 correspond to true minimum at potential energy surfaces. The input files were organized with the help of Gauss View 5 [24]. The Gauss View 5.0, Avogadro [25] and Chemcraft [26] programs were employed for interpreting output files.

2.4. Molecular Docking studies

2.4.1. Protein structure and newly synthesized compounds preparation

In molecular docking protocol, the X-ray structure of Jack bean urease (PDB ID 4H9M) was retrieved from Protein Data Bank (PDB) (https://www.rcsb.org/), prepared by using protein preparation wizard embedded in Schrodinger software (www.schrodinger.com). Protein preparation includes structure refinement, removal of unnecessary ligands, co-factors, water molecules, addition of missing residues (using Prime), and polar hydrogen atom. Ionization and states were also generated at PH 7. Finally structure was minimized by applying force field OPLS 2005 to remove steric hindrance and allowed deviation of 0.3 RMS from its native conformation. Synthesized compounds were drawn in Chem draw ultra and prepared using LigPrep tool in Schrodinger Release 2018-2. Stereoisomers and possible ionization states were generated by keeping at most 32 possible conformers of each compound.

2.4.2. Grid generation and Docking Protocol

Before docking the synthesized compounds, Grid box was generated around the Nickel ions present in the active site. Size of cubic box was set at 20Å in each dimension and X, Y, Z coordinates setting parameters which include cutoff radius scaling of 0.25 and Van der Waal factor 1.0 were defined at 17.5, 36.56, 20.48 respectively. After grid generation, the candidate compound was docked into the receptor grid using GLIDE standard precision mode (SP) to predict best binding mode of the competitive inhibitor. Initially 200 conformations were generated in the active site, out of which top five were minimized and finally best was selected based on the glide score.

3. Results and Discussion

3.1. Chemistry

The target benzenesulfonohydrazides (INS1-INS-5) were prepared by interaction of INS with *p*-toluenesulfonyl chloride and benzenesulfonyl chloride respectively and were resulted in good yield (75.5-94.2 %, Table 1). Synthetic route is depicted in scheme 1. All the synthesized compounds were

characterized by performing IR, UV, ^{1}HNMR, and ^{13}CNMR studies. In IR spectra, a broad absorption band at 3572-3242 cm^{-1} indicating the presence of -NH moiety of sulfonamides in while a strong absorption band in 1154-1158 cm^{-1} (symmetrical) while 1307-1337 cm^{-1} (asymmetrical)for all synthesized compounds confirm the presence of -NH-S=O group. Moreover, characteristics sulfoxide absorption band appeared in region 1089-1091cm^{-1} for all synthetic compounds. In ^{1}H NMR spectra, the peaks for –NH proton of –CONH- group appeared at δ 8.02-8.08 ppm whereas proton of –CH-pyridyl appeared at δ 8.89 ppm. The singlet at δ 2.32 ppm assigned to proton of $–CH_3$ linked to aryl. In addition, all the other aliphatic and aromatic protons appeared in appropriate values of chemical shifts. In ^{13}C NMR spectra, characteristics peaks at δ 164.2-165.8 ppm assigned to amide carbon (-CONH-) while signals for methyl carbon in all the compounds were appeared at δ 21.3 ppm. So, ^{13}C NMR spectral analyses were consistent with assigned structure of all compounds.

3.2. Urease inhibition

All the synthesized benzenesulfonohydrazides were evaluated for urease inhibitory activity using well known indophenol method. By using serial dilution method, 250-0.49µM concentrations were used of each synthetic compound, thiourea (standard inhibitor for urease) for inhibitory assay and also IC_{50} of each compound was calculated under investigation (Table 1). Compound INS-5 was found to be more potent (IC_{50}= 1.11±0.29µM) among the tested compounds, whereas INS-3 and INS-4 with same terminal aryl ring with and without $–CH_3$ group respectively exhibited equal urease inhibition.

Table 1. IC_{50} and kinetics parameters of benzenesulfonohydrazides

Compound	IC_{50} (µM); mean±SEM (% inhibition)	[a] $V_{max\ (app)}$ (µM/min)	[b] $K_{m\ (app)}$ (mM)	[c] K_i (µM)	Mode of inhibition
INS-1	1.79±0.18 (90.9)	8.68	6.19	4.32	Mixed
INS-2	1.33±0.14 (86.8)	7.21	3.07	5.60	Competitive
INS-3	4.89±0.09 (81.1)	-	-	-	-
INS-4	4.86±0.11 (81.3)	-	-	-	-
INS-5	1.11±0.29 (81.8)	7.00	11.05	2.76	Mixed
[d] Thiourea	15.51±0.11 (92.1)	18.61	2.18	18.18	Competitive

[a] $V_{max\ (app)}$= Maximum velocity of enzymatic activity at 20 µM inhibitor concentration

[b] $K_{m(app)}$= Michaelis–Menten constant at 20 µM inhibitor concentration

[c] K_i(µM)= Calculated from Dixon plot, [d] Standard inhibitor of urease

Inhibition mechanism was also investigated by performing the kinetic studies on three most potent compounds INS-1, INS-2 and INS-5 with different concentration of compounds (0-20 µM) and substrate (0.5-4.0 mM). Mode of inhibition and inhibition constant (K_i) were determined by enzymatic kinetics. Lineweaver Burk plots were used to assess the mode of inhibition by determining the effect of inhibitors (compounds) on V_{max} and K_m. V_{max} of jack bean urease enzyme was not effected in the presence of inhibitor (INS-2) while K_m of enzyme increase which indicate the competitive inhibition. The enzymatic kinetics of most active compound is presented below in Fig. 2-4.

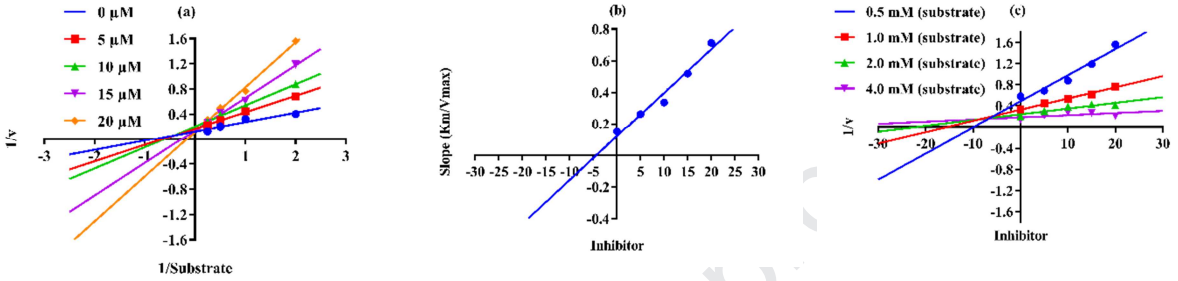

Fig. 2 Enzymatic kinetics of compound INS-1, (a) Lineweaver–Burk plot (b) Secondary replot (Lineweaver–Burk) (c) Dixon plot

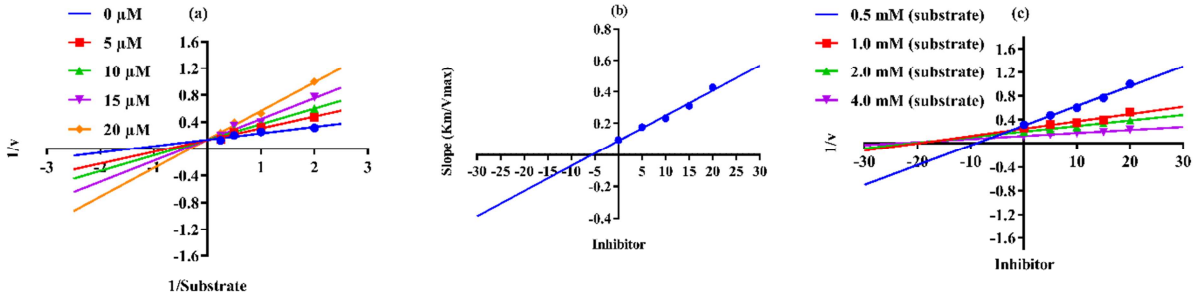

Fig. 3 Enzymatic kinetics of compound INS-2, (a) Lineweaver–Burk plot (b) Secondary replot (Lineweaver–Burk) (c) Dixon plot

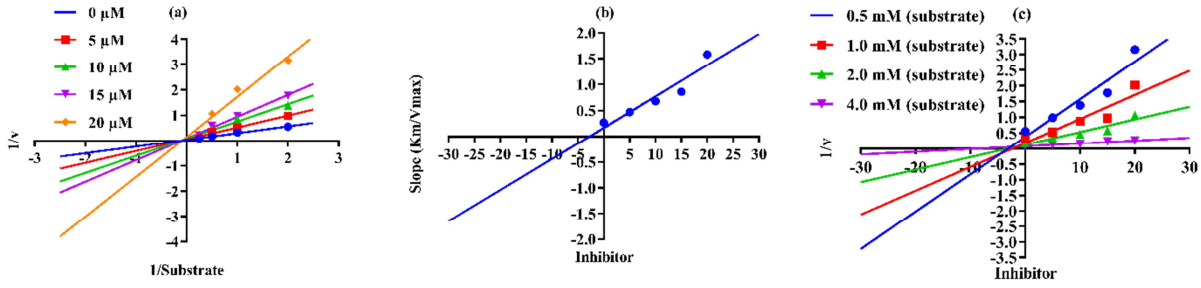

Fig. 4 Enzymatic kinetics of compound INS-5, (a) Lineweaver–Burk plot (b) Secondary replot (Lineweaver–Burk) (c) Dixon plot

Both V_{max} (decreased) and K_m (increased) of jack bean urease enzyme were affected in the presence of inhibitors (INS-1 and INS-5) which indicate the mixed type inhibition and these compounds could interact at the allosteric site or active site of the enzyme. Lineweaver Burk secondary plots were drawn between the slope of each line and different concentrations of inhibitors to calculate K_i values. Dixon plots were drawn between the reciprocal of rate of reaction and different concentration of inhibitors to confirm the K_i value of each inhibitor. It was concluded from kinetic studies that compound INS-2 was competitive inhibitor with Ki values (Table 1) 5.60 µM while the compounds INS-1 and INS-5 were mixed type of inhibitors with Ki values 4.32 and 2.76 µM respectively (Table 1).

Hydrazide moiety along with other cyclics, heterocyclics and sulfoxide explored for antiurease activities in literature. Isatin derived sulfonyl hydrazides [27], phosphorehydrazides [28] and benzohydrazides [29] revealed the IC_{50} values ranged between 39-148 µM, 1.611-7.251 µM and 0.87-19 µM respectively. But in the benzohydrazides series the compounds with IC_{50} values 1.64, 1.82 and 1.97 µM showed the competitive mode of inhibition. Whereas in this work the compound INS-2 showed competitive mode of inhibition with IC_{50} value 1.33 µM which is lower than reported compounds with same mode of inhibition.

3.3. Computational studies

All synthesized compounds (INS1-INS-5) are optimized by using density functional theory (DFT) at B3LYP level of theory and 6-311G(d,p) basis set conjunction. The optimized coordinates and dihedral angles of optimized geometries are presented in Supplementary data (Table S1-S6). The fully optimized geometries of all compounds are present in Fig.5a.

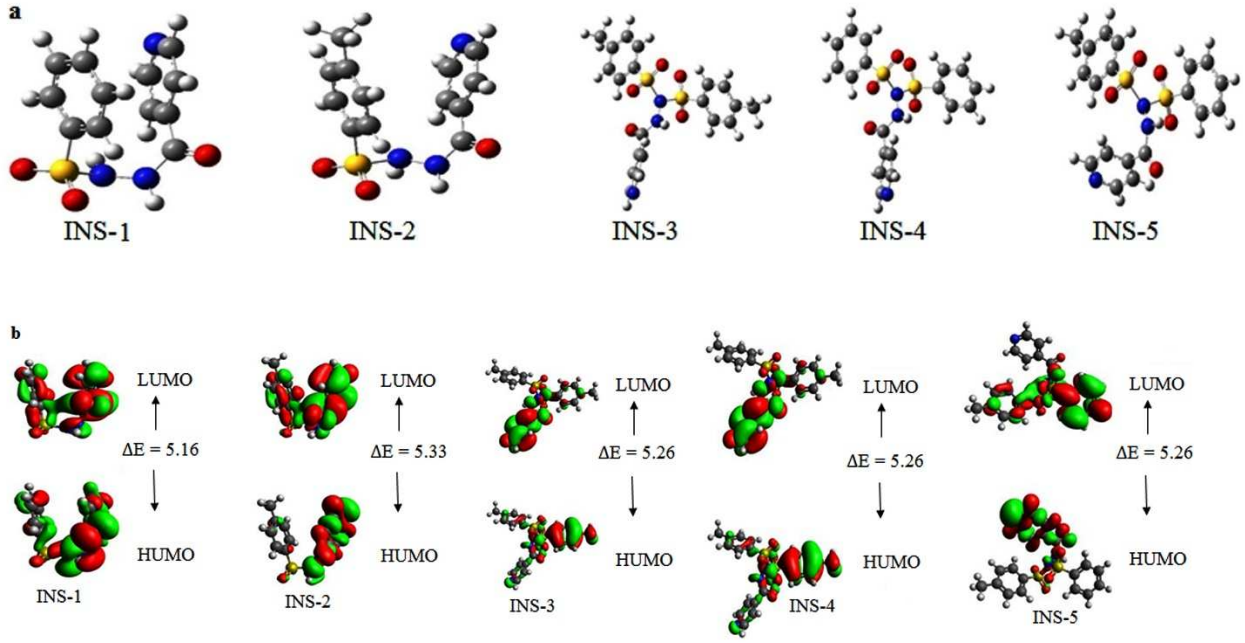

Fig. 5 Optimized geometries (a) calculated at B3LYP/6-311G(d,p) level of DFTand frontier molecular orbital (FMO's) diagrams (b) of synthesized compounds (INS-1-INS-5)

3.3.1. Frontier molecular orbital (FMO) analysis

Frontier molecular orbitals of investigated molecules are calculated at B3LYP/6-311G (d,p) level of theory and computed results are given in Fig. 5b and results are placed in Table S7 (supplementary data). In addition the discussion related to chemical reactivity and frontier molecular orbitals is also present in supplementary data. The energy gaps values of investigated compounds INS-1-INS-5 are found close to each other with only a minute difference. The smallest energy gap value among investigated compounds (INS-1-INS-5) is found to be in INS-1 with ΔE value of 5.16 eV. This might due to the planar configuration and absence of any additional functional group in INS-1 as compared to other architectures of compounds. In contrast, computational findings reflect that the highest ΔE value of 5.33 eV is observed in INS-2. Overall, the increasing order of HOMO-LUMO energy gap is noticed as: INS-1< INS-3 = INS-4 =INS-5 <INS-2. The pictorial representation is shown in Fig. 6 in which red color specifies the negative phase while green color indicates the positive phase of molecular orbitals respectively.

3.3.2. Global reactivity descriptors

Result of ionization potential and electron affinity mentioned in Table S8 (Supplementary Information) reveal that our compounds of interest INS-1-INS-5 show higher value of ionization potential as compared to electron affinity indicating the greater electron donating aptitude of INS-1-INS-5 as compared to their accepting nature. Overall, *A* value is found positive in all compounds which is a good indication for the possible utilization of these compounds in charge transfer reactions. Electrophilicity results also evident that electron donor capability (ω^-) values of all compounds are very large as compared to the electron accepting capability (ω^+) values. The global softness value is found to be greater and with third digit difference in INS-3, INS-4, INS-5, while smaller and one digit difference in INS-1, INS-2. Following decreasing order of electronegativity is observed among INS-1-INS-5 compounds INS-1>INS-4 >INS-2 >INS-5>INS-3. The studied compounds INS-1-INS-5 are found to be chemically hard in nature owing to larger values of global hardness as compared to global softness. These results unveil the great chemical stability and less reactivity. The value of chemical potential μ shows a direct relation with chemical stability and inverse relation with reactivity of the compounds under observation (INS-1-INS-5). In compounds under our investigation INS-1-INS-5, the following decreasing order of chemical potential is found: [INS-1 (μ = -4.762 *eV*)] > [INS-4 (μ = -4.724 *eV*)] > [INS-2 (μ = -4.683 *eV*)] > [INS-5 (μ = -4.636 *eV*)] > [INS-3 (μ = -4.558 *eV*)]. This order points out that compound INS-1 has lowest value of chemical potential (μ) which prove that it is the least stable and most reactive compound. This result is also in fine agreement with the HOMO-LUMO energy gap proving the fact that molecules with smaller Δ*E* value are considered as soft molecules with small kinetic stability, large reactivity. Overall findings of global reactivity parameters indicate that all investigated compounds contain more donating capability, stability and less accepting

aptitude. All studied compounds are suitable and can participate in charge transfer reactions. Furthermore, the actual reason for performing density functional theory (DFT) calculations is to support experimental and molecular docking studies and also countercheck the experimental findings along with evaluation of stability, reactivity, intra or intermolecular charge transfer that are useful parameters to provide clue for potential biological activities of studied compounds [32, 33]. For instance, Tables S7 and S8 results provide evident about softness, reactivity, accepting and donating aptitude of the investigated molecules which have good relationship with potential biological activities.

3.3.3. Natural bond orbital (NBO) analysis

The natural bond orbital (NBO) analysis is widely performed to investigate the different hyperconjugative and non-covalent interactions in the molecules [34, 35]. The NBO analysis is proved to be a helpful tool for examine the hydrogen bonding originates from hyper-conjugation. The NBO analysis is also used to determine the transfer of densities from filled orbitals (Lewis type NBOs orbitals) to unfilled or vacant orbitals (non-Lewis NBOs orbitals) of investigated molecules. In present study, we have made an attempt to investigate all above mentioned interactions in 5 compounds by using DFT calculations at B3LYP/6-311G (d,p) level of theory and results are summarized in Table 2. Following equation 1 is proved to be helpful in exploring the interactions and second order Fock Matrix.

$$E^2 = q_i \frac{(F_{i.j})^2}{\varepsilon_j - \varepsilon_i} \qquad (1)$$

Here E^2 represents stabilization energy, q_i represents donor orbital occupancy, $F_{i,j}$ describes off diagonal NBO Fock matrix elements and $\varepsilon_j, \varepsilon_i$ represents diagonal elements. The results obtained from NBO analysis is tabulated in Table 2. And atoms numbering of INS-1-INS-5 according to NBO charge is also present in Figure S1 (Supplementary data).

Table 2. Second-order perturbation theory analysis of Fock matrix on NBO basis for all compounds

Compound	Donor (i)	Type	Acceptor (j)	Type	E(2) [Kcal/mol][a]	E(j) E(i)[b][a.u.]	F(I;j)[c][a.u.]
	C_6-C_7	σ	C_7-N_9	σ*	0.53	1.08	0.022
	N_3-C_4	π	C_1-C_2	π*	25.14	0.32	0.081
INS-1	C_5-C_6	π	N_3-C_4	π*	26.49	0.28	0.077
	C_1-C_6	σ	C_5-H_{23}	σ*	2.90	1.14	0.051
	O_{12}	L.P[2]	N_9-N_{10}	σ*	0.51	0.61	0.161
	N_9	L.P[1]	C_7-O_8	π*	28.26	0.38	0.093
	N_{10}-H_{26}	σ	N_{10}-S_{11}	σ*	0.53	0.75	0.019
	C_{18}-C_{19}	π	C_{16}-C_{17}	π*	22.11	0.29	0.072
INS-2	C_{16}-C_{17}	π	C_{14}-C_{15}	π*	26.72	0.27	0.076
	C_5-C_6	σ	C_1-H_{21}	σ*	2.87	1.15	0.051
	N_{10}	L.P[1]	C_{14}-C_{15}	π*	0.55	0.39	0.014
	N_9	L.P[1]	C_7-O_8	π*	33.23	0.36	0.098
	S_{11}-O_{13}	σ	C_3-C_4	σ*	0.51	1.29	0.024
	C_{17}-C_{18}	π	C_{14}-C_{19}	π*	26.67	0.26	0.076
	C_{26}-C_{27}	π	C_{24}-C_{25}	π*	26.97	0.27	0.076
INS-3	C_{17}-C_{18}	σ	C_{20}-H_{24}	σ*	2.99	0.65	0.044
	N_{10}	L.P[1]	C_{24}-C_{25}	π*	0.57	0.34	0.013
	N_9	L.P[1]	C_7-O_8	π*	47.19	0.32	0.110
	S_{11}-O_{13}	σ	C_3-C_4	σ*	0.50	1.29	0.024
	C_{26}-C_{27}	π	C_{23}-C_{28}	π*	25.06	0.27	0.074
INS-4	C_5-C_6	π	N_3-C_4	π*	26.27	0.28	0.076
	C_1-C_6	σ	C_5-H_{32}	σ*	2.85	1.14	0.051
	N_9	L.P[1]	S_{11}-O_{13}	σ*	0.53	0.58	0.016
	N_9	L.P[1]	C_7-O_8	π*	46.84	0.32	0.110
	S_{21}-O_{22}	σ	S_{21}-O_{23}	σ*	0.52	1.15	0.020
	C_1-C_2	π	C_5-C_6	π*	22.47	0.29	0.073
INS-5	C_{16}-C_{17}	π	C_{24}-C_{15}	π*	27.71	0.27	0.077
	C_{16}-C_{17}	σ	C_{20}-H_{21}	σ*	2.76	0.65	0.042
	N_{10}	L.P[1]	C_5-C_6	π*	0.54	0.41	0.014
	O_{13}	L.P[3]	N_{10}-S_{11}	σ*	27.38	0.32	0.087

[a] Mean energy of hyper conjugative,

[b] Energy difference between donor and acceptor i and j NBO orbitals

[c] Fock matrix element between i and j NBO orbitals

NBO analysis suggests four different types of transitions in molecules which are $\sigma \rightarrow \sigma^*$, $\pi \rightarrow \pi^*$, L.P$\rightarrow\sigma^*$ and L.P$\rightarrow\pi^*$. The intra-molecular hydrogen bonding also plays a vital role in stabilizing the molecule. The $\pi \rightarrow \pi^*$ transition in molecules confirms the conjugations. The dominant $\pi \rightarrow \pi^*$ transitions in INS-1-INS-5 are found to be as $\pi(C_5\text{-}C_6) \rightarrow \pi^*(N_3\text{-}C_4)$, $\pi(C_{16}\text{-}C_{17}) \rightarrow \pi^*(C_{14}\text{-}C_{15})$, $\pi(C_{26}\text{-}C_{27}) \rightarrow \pi^*(C_{24}\text{-}C_{25})$, $\pi(C_5\text{-}C_6) \rightarrow \pi^*(N_3\text{-}C_4)$ and $\pi(C_{16}\text{-}C_{17}) \rightarrow \pi^*(C_{24}\text{-}C_{15})$ with stabilization energy values of 26.49, 26.72, 26.97, 26.27 and 26.71 Kcal/mol respectively. In case of resonance large values of stabilization energy is seen, which suggests the delocalization of electrons of oxygen and nitrogen atoms to the entire system. These transitions are L.P (N_9) $\rightarrow \pi^*$ (C_7-O_8) in INS-1, L.P (N_9) $\rightarrow \pi^*$ (C_7-O_8) in INS-2, L.P (N_9)$\rightarrow \pi^*$(C_7-O_8) in INS-3, L.P(N_9)$\rightarrow \pi^*$(C_7-O_8) in INS-4 and L.P (O_{13})$\rightarrow \sigma^*$(N_{10}-S_{11}) in INS-5 with stabilization energy of 28.26, 33.23, 47.19, 46.84 and 27.38 Kcal/mol respectively. Moreover, in all compounds hydrogen bonding due to hyper conjugation is also present and relevant data is enclosed in Table 2. Similarly, Table 2 results confirmed that successful intramolecular charge transfer (ICT) due to delocalization of electrons on whole systems and hyper-conjugative interactions (HCIs) among bonds provide stability to the investigated compounds INS-1-INS 5.Furthermore, Table 2 results suggested that ICT and HCIs plays a crucial role for potential biological activities. In this way, Tables 2 results are supportive analysis for biological potential of investigated molecules. From preceding discussion, it can be concluded that extended conjugation is present in all compounds INS-1-INS-5. Successful intramolecular charge transfer due to delocalization of electrons on whole systems and hyper-conjugative interactions (HCIs) among bonds provide stability to the investigated compounds INS-1-INS-5.

3.3.4. FT-IR analysis

Nowadays, modern vibrational spectroscopy is proved to be helpful tool for identifying the modes of vibration in investigated compounds (experimental as well as theoretical)[36]. Experimentally FT-IR spectrum is recorded in the range of 4000-600 cm^{-1} while theoretically spectrum with harmonic frequencies, nature of vibrational modes and intensities of the vibrational bands for compounds INS-1-INS-5was examined by utilizing DFT/B3LYP/6-311G(d,p) level of theory. The most important experimental and theoretical FT-IR descriptions with concerning assignment are presented in Table S9 (Supplementary data).

3.3.4.1. C–H vibrations

DFT computed and experimentally recorded frequency bands unveils that the C-H vibrational bands are mostly observed due to wagging, scissoring, twisting and rocking mode of vibrations. In INS-1, twisting and rocking mode of vibration is observed at wave numbers 898, 1007, 1089 and 1215 cm^{-1} in benzene unit and 669 cm^{-1} in pyridine unit which show a good agreement with experimentally reported band at 907, 1001, 1091, 1236 cm^{-1} in benzene and 670 cm^{-1} in pyridine unit respectively. In INS-2 compound, rocking mode of vibration is observed at wave number 1141, 1228 cm^{-1} in benzene unit and 1092, 3225 cm^{-1} in pyridine unit which correlate with experimentally reported *C-H* band

found at 1157, 1223 cm^{-1} in benzene and 1090, 3244 cm^{-1} in pyridine unit correspondingly. In INS-3, C-H vibrational band in benzene is recorded at 1336 cm^{-1} and in pyridine ring at 1092, 1226 cm^{-1} which show a good harmony with experimentally reported *C-H* band at 1336 cm^{-1} in benzene unit and 1089, 1225 cm^{-1} in pyridine ring respectively. In INS-4 and INS-5 compound, theoretically *C-H* vibrational band is recorded at 1528 cm^{-1} and 1143, 3228 cm^{-1} in benzene and pyridine rings respectively. These theoretically calculated values show a good harmony with experimentally reported band at 1540 cm^{-1} and 1156, 3248 cm^{-1} in compound INS-4 and INS-5 respectively. In pyridine unit *C-H* vibrational band is recorded at wave numbers 1095, 1528 cm^{-1} in INS-4 and at wave numbers 1094, 1337 cm^{-1} in INS-5. These values show correlation with experimentally recorded *C-H* vibrational bands at wave number 1090, 1528 cm^{-1} (INS-4) and 1090, 1337 cm^{-1} (INS-5) respectively.

3.3.4.2. C-C stretching vibration

In current report, C-C stretching vibrations are found mostly in benzene rings and pyridine units. The C-C vibrational bands are seen in the benzene ring with stretching frequencies at wave number 1042 cm^{-1} (INS-1), 1141, 1339, 1615 cm^{-1} (INS-2), 847, 1336 cm^{-1} (INS-3), 628 cm^{-1} (INS-4) and 1137 cm^{-1} (INS-5) which are associated nicely with experimental analyzed bands appeared at wave number 1058 cm^{-1} (INS-1), 1157, 1337, 1603 cm^{-1} (INS-2), 845, 1336 cm^{-1} (INS-3), 634 cm^{-1} (INS-4) and 1136 cm^{-1} (INS-5) respectively. Similarly, in pyridine units of all compounds, vibrational bands with stretching frequencies observed in 1324 cm^{-1} (INS-1), 1013 cm^{-1} (INS-2), 1010 cm^{-1} (INS-3), 1010 cm^{-1} (INS-4) and 1596 cm^{-1} (INS-5) show excellent consistency with experimental vibrational band appeared at 1307, 1001, 1001, 1001 and 1595 cm^{-1} respectively.

3.3.4.3. N-H band vibration

N-H stretching vibrational mode in INS-1 are noticed with wave number at 669 cm^{-1}, in INS-2 at 902, 3500 cm^{-1}, in INS-3 at 3571 cm^{-1}, in INS-4 at 3572 cm^{-1} and in INS-5 at 631 cm^{-1} which shows a nice concurrence with experimental observed frequencies at 670, 906, 3537, 3565, 3572 and 632 cm^{-1} respectively. From preceding discussion, it is well evident that the experimental and computed FT-IR results are in very good agreement with each other.

3.4. UV-Visible study

Ultraviolet-Visible (UV–Vis)spectroscopy is a very useful tool for estimating the nature of electronic transition, probability of charge shifting within the compound and molecular assignment according to transition[37]. UV-Visible study is performed experimentally as well as theoretically by using specific tools. Theoretically UV-Visible study is performed by using time-dependent DFT (TDDFT) at B3LYP/6-311G(d,p) level of theory. TDDFT computed spectral results with experimental absorption spectral results, oscillator strength (*f*) and concern molecular orbital contributions in compounds INS1-INS5 is tabulated in Table 3. Results of maximum absorption for all compounds obtained from experimental and computational analysis are found very close to each other. The computed UV-

Visible spectra of INS1 highlighted λ_{max} at 242.84 nm with oscillating strength value of 0.05. In compound INS-2 and INS-3 λ_{max} is observed at 248.40 nm and 248.09 nm with oscillating strength value 0.01, 0.01 and E^{DFT} values of 2.5800 and 0.0008 respectively. The simulated λ_{max} and *f* in compound INS-4 are found closer to INS-1, INS-2 and INS-3 with values of 243.92 nm, 0.01 respectively. The computed UV-Visible spectra of INS-5 showed λ_{max} at 244.54 nm with oscillating strength value of 0.06. Overall, calculated UV-Visible spectrum of INS, INS2, INS-3, INS-4 and INS-5 showed absorption maximum at 242.84, 248.40, 248.09, 243.92 and 244.54 nm which is in reasonable agreement with the experimental UV-Visible spectrum valued observed at 242, 242, 235, 235, 242 nm respectively. HOMO to LUMO electronic transition which is the characteristic of soft molecules, hence, may have potential of utilization in biological applications.

Table 3. Absorption values (λ_{max}), oscillator strength (*f*), are calculated at TDDFT/B3LYP/6-31G(d,p) level of theory in the methanol solvent

Compounds	Cal. λ_{max} (nm)	Exp. λ_{max} (nm)	*f* (oscillator strength)	MO contributions
INS-1	242.84	242	0.05	H→L+1(81%)
INS-2	248.40	242	0.01	H-3→L (88%)
INS-3	248.09	235	0.01	H-6→L (24%), H-5→L (25%), H-3→L (11%)
INS-4	243.92	235	0.01	H-3→L (20%), H-2→L (42%)
INS-5	244.54	242	0.06	H-3→L (25%), H-2→L (31%), H→L (12%)

3.5. Molecular electrostatic potential (MEP) analysis

Three dimensional plot of electron density on whole compound is investigated through molecular electrostatic potential analysis using following equation 2.

$$V(r) = \sum(\frac{Z_A}{R_A} - r) - \int(p(r')/r' - r)dr' \quad (2)$$

In above equation V(r) represents molecular electrostatic potential and Z_A represents charge density over nucleus. A placed at RA, *p*(r') defines the electronic density function and r' is the integration variable[38, 39]. The color in MEP analysis actually defines the sites for electrophilic and nucleophilic attack. Electrostatic potential magnitude is increasing in following order; red < orange < yellow <green < blue[40]. The red color represents the best site for electrophilic attack and blue color indicates the site which is best for nucleophilic attack. So, for the MEP analysis were formed at

B3LYP/6-311G(d,p) functional for INS-1-INS-5and results are portrayed in Fig. 6. It can be seen that negative potential (red color) is shown by oxygen atoms, while blue area shows positive potential exhibited mostly by nitrogen and partially by hydrogen and carbon atoms. But green area shows mean potential i.e. the area between two extremes. From red and blue colors it is cleared that different reaction sites are presents in all molecules.

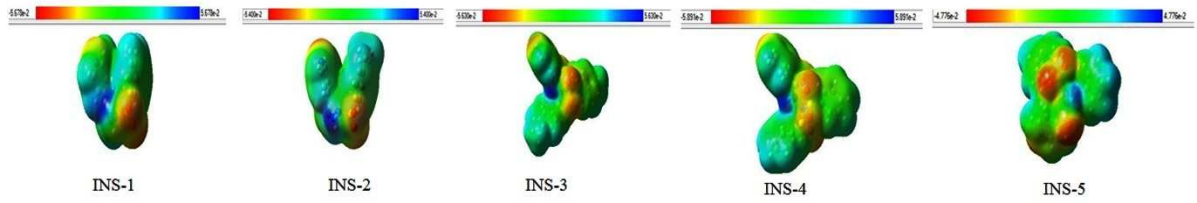

Fig. 6 Molecular electrostatic potential of compounds at DFT/B3LYP/6-311G(d,p) basis set

3.6. Binding mode prediction using molecular docking studies

The competitive inhibitor INS-2 was docked in the active site of urease enzyme as shown in Fig. 7. The pyridine ring directed towards the zinc metal ion is making an electrostatic interaction shown in Fig. 7b. The MEP analysis also show that N present in the pyridine has strong tendency for nucleophilic attack which might be responsible for making observed pose of INS-2 compound as shown in Fig. 7a. The tail part containing the toluene moiety is exposed towards the solvent side, contributing to push the compound in active site. The compound has gorged well in the binding site also making t-type π-π interactions with HIS-519 and HIS-492 residues which might be responsible for making it competitive inhibitor.

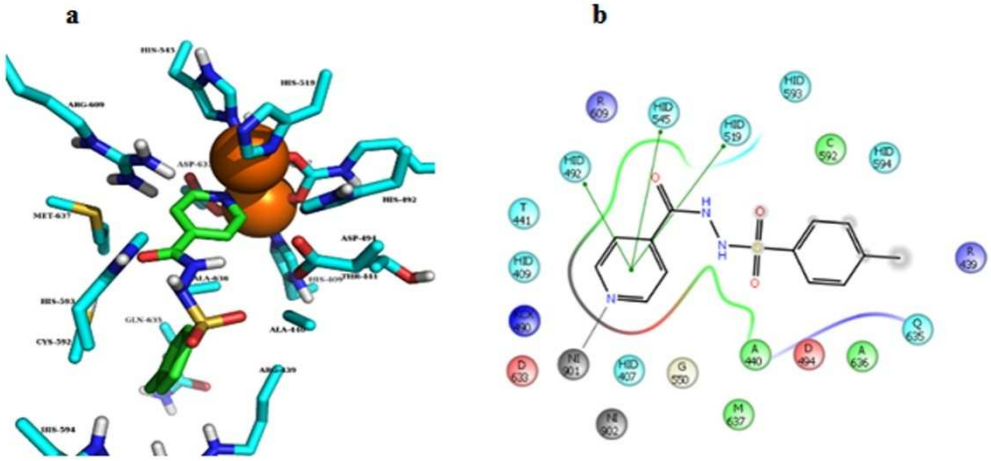

Fig. 7 Binding mode of competitive inhibitor (INS-2) in urease enzyme. a) Best docked pose of INS-2 compound (green sticks) in urease active site (cyan sticks), Nickle ions are mentioned with brown sphere. b) 2D view of INS-2 docking pose in active site.

Conclusion

In this study, five hydrazides were successfully synthesized and their structures were confirmed by physiochemical and spectral techniques. All the compounds were assayed for in vitro urease inhibition studies. Among the tested compounds, compound INS-5 exhibited lowest IC_{50} value (1.11±0.29 µM) and other compounds in the series showed good antiurease activity. Inhibition mechanisms (competitive, mixed or non-competitive) of biologically assayed compounds were also investigated by Lineweaver Burk and Dixon plots to determine the V_{max}, K_m and K_i values. Among the already reported benzohydrazides [29], compounds with IC_{50} values 1.64, 1.82 and 1.97 µM showed the competitive mode of inhibition whereas in this work the compound INS-2 showed competitive mode of inhibition with IC_{50} values 1.33 µM which is lower than reported compounds with same mode of inhibition. The experimental FT-IR and UV-Visible spectroscopic analysis showed reasonable agreement to corresponding DFT based results. The NBO analysis confirmed that the presence of hyperconjugative interactions and intramolecular charge transfer are pivotal cause for the existence of stability of investigated compounds. Global reactivity parameters indicate that INS-1-INS-5 contain more donating capability, stability and less accepting aptitude. MEP descriptor indicates that oxygen atoms in all title compounds are prone to electrophilic attack, while nitrogen and carbon atoms are prone to nucleophilic attack which is also evident in docking studies of competitive inhibitor. We hope that this synergistic experimental-computational study may provide new ways for the utilization of INS-1-INS-5 in biological chemistry.

Acknowledgment

The authors are thankful to HEC-Pakistan for providing financial support to purchase software and hardware for computational studies vide Projects No. 6804/Federal/NRPU/R&D/HEC/2016 & 8094/Balochistan/NRPU/R&D/HEC/2017.

References

[1] W.-K. Shi, R.-C. Deng, P.-F. Wang, Q.-Q. Yue, Q. Liu, K.-L. Ding, M.-H. Yang, H.-Y. Zhang, S.-H. Gong, M. Deng, 3-Arylpropionylhydroxamic acid derivatives as Helicobacter pylori urease inhibitors: Synthesis, molecular docking and biological evaluation, Bioorg. Med. Chem. 24(19) (2016) 4519-4527.

[2] A. Hameed, K.M. Khan, S.T. Zehra, R. Ahmed, Z. Shafiq, S.M. Bakht, M. Yaqub, M. Hussain, A.d.l.V. de León, N. Furtmann, Synthesis, biological evaluation and molecular docking of N-phenyl thiosemicarbazones as urease inhibitors, Bioorg. Chem. 61 (2015) 51-57.

[3] C. Follmer, Ureases as a target for the treatment of gastric and urinary infections, J. Clin. Pathol. 63(5) (2010) 424-430.

[4] M. Imran, S. Waqar, K. Ogata, M. Ahmed, Z. Noreen, S. Javed, N. Bibi, H. Bokhari, A. Amjad, M. Muddassar, Identification of novel bacterial urease inhibitors through molecular shape and structure based virtual screening approaches, RSC Advances 10(27) (2020) 16061-16070.

[5] K.A. Eaton, C. Brooks, D. Morgan, S. Krakowka, Essential role of urease in pathogenesis of gastritis induced by Helicobacter pylori in gnotobiotic piglets, Infect. Immun. 59(7) (1991) 2470-2475.

[6] K. Stingl, K. Altendorf, E.P. Bakker, Acid survival of Helicobacter pylori: how does urease activity trigger cytoplasmic pH homeostasis?, Trends Microbiol. 10(2) (2002) 70-74.

[7] P. Krishnamurthy, M. Parlow, J.B. Zitzer, N.B. Vakil, H.L. Mobley, M. Levy, S.H. Phadnis, B.E. Dunn, Helicobacter pylori containing only cytoplasmic urease is susceptible to acid, Infect. Immun. 66(11) (1998) 5060-5066.

[8] M.W. Pinkse, C.S. Maier, J.I. Kim, B.H. Oh, A.J. Heck, Macromolecular assembly of Helicobacter pylori urease investigated by mass spectrometry, J. Mass Spectrom. 38(3) (2003) 315-320.

[9] D.J. Evans Jr, D.G. Evans, S.S. Kirkpatrick, D.Y. Graham, Characterization of the Helicobacter pylori urease and purification of its subunits, Microb. Pathog. 10(1) (1991) 15-26.

[10] A. Rauf, S. Shahzad, M. Bajda, M. Yar, F. Ahmed, N. Hussain, M.N. Akhtar, A. Khan, J. Jończyk, Design and synthesis of new barbituric-and thiobarbituric acid derivatives as potent urease inhibitors: Structure activity relationship and molecular modeling studies, Bioorg. Med. Chem. 23(17) (2015) 6049-6058.

[11] Y. Gull, N. Rasool, M. Noreen, A. Altaf, S. Musharraf, M. Zubair, F.-U.-H. Nasim, A. Yaqoob, V. DeFeo, M. Zia-Ul-Haq, Synthesis of N-(6-Arylbenzo [d] thiazole-2-acetamide derivatives and their biological activities: an experimental and computational approach, Molecules 21(3) (2016) 266.

[12] L.V. Modolo, A.X. de Souza, L.P. Horta, D.P. Araujo, A. de Fatima, An overview on the potential of natural products as ureases inhibitors: A review, J. Adv. Res. 6(1) (2015) 35-44.

[13] M. Taha, S.A.A. Shah, A. Khan, F. Arshad, N.H. Ismail, M. Afifi, S. Imran, M.I. Choudhary, Synthesis of 3, 4, 5-trihydroxybenzohydrazone and evaluation of their urease inhibition potential, Arab. J. Chem. 12(8) (2019) 2973-2982.

[14] K.M. Khan, M. Irfan, M. Ashraf, M. Taha, S.M. Saad, S. Perveen, M.I. Choudhary, Synthesis of phenyl thiazole hydrazones and their activity against glycation of proteins, Med. Chem. Res. 24(7) (2015) 3077-3085.

[15] K.M. Khan, F. Rahim, A. Wadood, M. Taha, M. Khan, S. Naureen, N. Ambreen, S. Hussain, S. Perveen, M.I. Choudhary, Evaluation of bisindole as potent β-glucuronidase inhibitors: Synthesis and in silico based studies, Bioorg. Med. Chem. Lett. 24(7) (2014) 1825-1829.

[16] J.D. Kendall, G.W. Rewcastle, R. Frederick, C. Mawson, W.A. Denny, E.S. Marshall, B.C. Baguley, C. Chaussade, S.P. Jackson, P.R. Shepherd, Synthesis, biological evaluation and molecular modelling of sulfonohydrazides as selective PI3K p110α inhibitors, Bioorg. Med. Chem. 15(24) (2007) 7677-7687.

[17] K.G. Krishnan, P. Ashothai, K. Padmavathy, W.-M. Lim, C.-W. Mai, P.V. Thanikachalam, C. Ramalingan, Hydrazide-integrated carbazoles: synthesis, computational, anticancer and molecular docking studies, New J. Chem. 43(30) (2019) 12069-12077.

[18] R.M. Mohareb, K.A. EL-Sharkawy, F.O. Al Farouk, Synthesis, cytotoxicity against cancer and normal cell lines of novel hydrazide–hydrazone derivatives bearing 5H-chromen-5-one, Med. Chem. Res. 28(11) (2019) 1885-1900.

[19] M.A. Qadir, M. Ahmed, H. Aslam, S. Waseem, M.I. Shafiq, Amidine Sulfonamides and Benzene Sulfonamides: Synthesis and Their Biological Evaluation, J. Chem. 2015 (2015) 8.

[20] M.A. Qadir, M. Ahmed, M. Iqbal, Synthesis, characterization, and antibacterial activities of novel sulfonamides derived through condensation of amino group containing drugs, amino acids, and their analogs, BioMed Res. Int. 2015 (2015) 7.

[21] M.A. Qadir, M. Ahmed, A. Khaleeq, Synthesis and biological evaluation of amino terminal modified new sulfonamides of contemporary drugs, Lat. Amer. J. Pharm. 34(4) (2015) 719-724.

[22] M. Ahmed, M.A. Qadir, A. Hameed, M.N. Arshad, A.M. Asiri, M. Muddassar, Azomethines, isoxazole, N-substituted pyrazoles and pyrimidine containing curcumin derivatives: Urease inhibition and molecular modeling studies, Biochem. Biophys. Res. Commun. 490(2) (2017) 434-440.

[23] M. Frisch, G. Trucks, H. Schlegel, G. Scuseria, M. Robb, J. Cheeseman, G. Scalmani, V. Barone, B. Mennucci, G. Petersson, Gaussian09 Revision D. 01, Gaussian Inc. Wallingford CT, See also: URL: http://www. gaussian. com (2009).

[24] R. Dennington, T. Keith, J.G. Millam, version 5; Semichem Inc, Shawnee Mission, KS (2009).

[25] M.D. Hanwell, D.E. Curtis, D.C. Lonie, T. Vandermeersch, E. Zurek, G.R. Hutchison, Avogadro: an advanced semantic chemical editor, visualization, and analysis platform, J. Cheminformatics 4(1) (2012) 17.

[26] G.A. Andrienko, Chemcraft. Graphical Software for Visualization of Quantum Chemistry Computations, 2010.

[27] M. Arshad, M. Jadoon, Z. Iqbal, M. Fatima, M. Ali, K. Ayub, A.M. Qureshi, M. Ashraf, M.N. Arshad, A.M. Asiri, Synthesis, molecular structure, quantum mechanical studies and urease inhibition assay of two new isatin derived sulfonylhydrazides, J. Mol. Struct. 1133 (2017) 80-89.

[28] L. Asadi, K. Gholivand, K. Zare, Phosphorhydrazides as urease and acetylcholinesterase inhibitors: biological evaluation and QSAR study, Journal of the Iranian Chemical Society 13(7) (2016) 1213-1223.

[29] A. Abbas, B. Ali, K.M. Khan, J. Iqbal, S. Ur Rahman, S. Zaib, S. Perveen, Synthesis and in vitro urease inhibitory activity of benzohydrazide derivatives, in silico and kinetic studies, Bioorg. Chem. 82 (2019) 163-177.

[30] M.U. Khan, M. Khalid, M. Ibrahim, A.A.C. Braga, M. Safdar, A.A. Al-Saadi, M.R.S.A. Janjua, First theoretical framework of triphenylamine–dicyanovinylene-based nonlinear optical dyes: structural modification of π-linkers, J. Phys. Chem. C 122(7) (2018) 4009-4018.

[31] M.R.S.A. Janjua, M. Amin, M. Ali, B. Bashir, M.U. Khan, M.A. Iqbal, W. Guan, L. Yan, Z.M. Su, A DFT Study on The Two-Dimensional Second-Order Nonlinear Optical (NLO) Response of Terpyridine-Substituted Hexamolybdates: Physical Insight on 2D Inorganic–Organic Hybrid Functional Materials, Eur. J. Inorg. Chem. 2012(4) (2012) 705-711.

[32] R. Pardasani, P. Pardasani, V. Chaturvedi, S. Yadav, A. Saxena, I. Sharma, Theoretical and synthetic approach to novel spiroheterocycles derived from isatin derivatives and L-proline via 1, 3-dipolar cycloaddition, Heteroatom Chemistry: An International Journal of Main Group Elements 14(1) (2003) 36-41.

[33] F.A. Pasha, M.M. Neaz, S.J. Cho, S.B. Kang, Quantitative structure activity relationship (QSAR) study of estrogen derivatives based on descriptors of energy and softness, Chem. Biol. Drug Des. 70(6) (2007) 520-529.

[34] M. Khalid, M.A. Ullah, M. Adeel, M.U. Khan, M.N. Tahir, A.A.C. Braga, Synthesis, crystal structure analysis, spectral IR, UV–Vis, NMR assessments, electronic and nonlinear optical properties of potent quinoline based derivatives: interplay of experimental and DFT study, Journal of Saudi Chemical Society 23(5) (2019) 546-560.

[35] R. Jawaria, M. Hussain, M. Khalid, M.U. Khan, M.N. Tahir, M.M. Naseer, A.A.C. Braga, Z. Shafiq, Synthesis, crystal structure analysis, spectral characterization and nonlinear optical exploration of potent thiosemicarbazones based compounds: a DFT refine experimental study, Inorg. Chim. Acta 486 (2019) 162-171.

[36] M. Akram, M. Adeel, M. Khalid, M.N. Tahir, M.U. Khan, M.A. Asghar, M.A. Ullah, M. Iqbal, A combined experimental and computational study of 3-bromo-5-(2, 5-difluorophenyl) pyridine and 3, 5-bis (naphthalen-1-yl) pyridine: Insight into the synthesis, spectroscopic, single crystal XRD, electronic, nonlinear optical and biological properties, J. Mol. Struct. 1160 (2018) 129-141.

[37] R. Hussain, M.U. Khan, M.Y. Mehboob, M. Khalid, J. Iqbal, K. Ayub, M. Adnan, M. Ahmed, K. Atiq, K. Mahmood, Enhancement in Photovoltaic Properties of N, N-diethylaniline based Donor Materials by Bridging Core Modifications for Efficient Solar Cells, ChemistrySelect 5(17) (2020) 5022-5034.

[38] N. Okulik, A.H. Jubert, Theoretical analysis of the reactive sites of non-steroidal anti-inflammatory drugs, Internet Electron. J. Mol. Des. 4(1) (2005) 17-30.

[39] S. Muthu, A. Prabhakaran, Vibrational spectroscopic study and NBO analysis on tranexamic acid using DFT method, Spectrochim. Acta. A: Mol. Biomol. Spectrosc. 129 (2014) 184-192.

[40] G. Mahalakshmi, V. Balachandran, NBO, HOMO, LUMO analysis and vibrational spectra (FTIR and FT Raman) of 1-Amino 4-methylpiperazine using ab initio HF and DFT methods, Spectrochim. Acta. A: Mol. Biomol. Spectrosc. 135 (2015) 321-334.

Highlights

1. New Benzenesulfonohydrazide were synthesized and urease enzyme inhibition was evaluated through in vitro assays.
2. All compounds displayed potent urease inhibitory activity with IC_{50} values of 1.11–4.89 µM, the compound INS-2 was competitive inhibitor with Ki values 5.60 µM.
3. Molecular docking studies were established to elucidate the binding energy and interaction.
4. DFT and TDDFT calculations at B3LYP/6-311G(d,p) level of theory were performed, overall, experimental findings were supported nicely by corresponding DFT computed results.

Compliance with Ethical Standards

Informed consent: Not applicable

Conflict of interest: We wish to confirm that there are no known conflicts of interest associated with this publication.

Funding: There has been no financial support for this work that could have influenced its outcome.